High Resolution Focusing Analysis and Inversion for Small Scatterer Detection

Norman Bleistein
Center for Wave Phenomena
Colorado School of Mines
Golden, CO 80401-1887
phone: 303 273-3557, 3461 fax: 303 273-3478 norm@dix.mines.edu
Award Number: N00014-95-1-0508
http://www.cwp.mines.edu/~norm

LONG-TERM GOAL

The long-term goal of this project is to develop software to invert acoustic data from a towed source/receiver array for simultaneous velocity analysis, detection and material characterization of small-scale (7 to 15 cm) scatterers in the shallow ocean and seabed sediments. Detection will be achieved by providing a reflector map of the target region. Material characterization is provided through estimates of angularly dependent reflection coefficients at the surface of the target over multiple angles; angle versus offset analysis provides a basis for characterizing the internal material parameters of the target.

OBJECTIVES

The immediate objective is to complete the development of a computer code for towed array data that back propagates the data with a wavespeed that varies in all three spatial variables. This software is also to be integrated with software to carry out *velocity analysis* so that the change in wavespeed from the water column to the seabed can be properly treated. The more long-term objectives are to continue to incorporate developments in the underlying theory into the software being developed for this application. For example, the theory is currently being extended to *multi-pathing*---the case in which the ray trajectories from a point scatterer at depth form caustics in the subsurface, leading to multiple arrivals at the same observation point on the receiver array.

APPROACH

The particular experiment that is proposed requires the acquisition of acoustic responses along a towed array (about 10m) of sonophones from a single point source. The experiment is to be repeated on a regular near-surface areal grid. Our methods are based on a high frequency asymptotic inversion technique that is called *Kirchhoff inversion.* This method back projects the observed data through integration (summation) over diffraction traveltime curves that pick out the observed data on different traces at the indicated traveltimes. The distinctive feature of our approach is that we obtain an estimate of the specular reflection coefficient and specular incidence angle from the peak amplitude(s) of the output. These estimates are model-consistent (back-projection wavespeed) and require amplitude control of the source signature. On other scales, this method has achieved great success in seismic exploration, with lengths two-to-three orders of magnitude higher- and frequencies, correspondingly, two-to-three orders of magnitude lower- than those used for the experiments here. The method also has application to flaw characterization in solids---*nondestructive testing and evaluation.*

Report Documentation Page

Form Approved
OMB No. 0704-0188

1. REPORT DATE **30 SEP 1999**	2. REPORT TYPE	3. DATES COVERED **00-00-1999 to 00-00-1999**

4. TITLE AND SUBTITLE **High Resolution Focusing Analysis and Inversion for Small Scatterer Detection**	5a. CONTRACT NUMBER 5b. GRANT NUMBER 5c. PROGRAM ELEMENT NUMBER
6. AUTHOR(S)	5d. PROJECT NUMBER 5e. TASK NUMBER 5f. WORK UNIT NUMBER
7. PERFORMING ORGANIZATION NAME(S) AND ADDRESS(ES) **Colorado School of Mines,Center for Wave Phenomena,Golden,CO,80401-1887**	8. PERFORMING ORGANIZATION REPORT NUMBER
9. SPONSORING/MONITORING AGENCY NAME(S) AND ADDRESS(ES)	10. SPONSOR/MONITOR'S ACRONYM(S) 11. SPONSOR/MONITOR'S REPORT NUMBER(S)

12. DISTRIBUTION/AVAILABILITY STATEMENT
Approved for public release; distribution unlimited

13. SUPPLEMENTARY NOTES

14. ABSTRACT

15. SUBJECT TERMS

16. SECURITY CLASSIFICATION OF:			17. LIMITATION OF ABSTRACT	18. NUMBER OF PAGES	19a. NAME OF RESPONSIBLE PERSON
a. REPORT **unclassified**	b. ABSTRACT **unclassified**	c. THIS PAGE **unclassified**	**Same as Report (SAR)**	**5**	

Standard Form 298 (Rev. 8-98)
Prescribed by ANSI Std Z39-18

WORK COMPLETED

We have previously delivered software to process such data under the assumption that the shallow water and seabed environment was a medium with a wavespeed that was only depth dependence; first a 2.5D code was developed, then a 3D code. The designation, 2.5D, refers to three dimensional wave propagation over an ocean and seabed model that is assumed to have two-dimensional variability, only. This technique allows the processing of a single line of data, producing a hybrid output that still honors three-dimensional propagation properties--in particular, three-dimensional geometrical spreading of the amplitude. The current software uses a full areal survey and allows for three-dimensional variation in the background wavespeed. It also will produce three-dimensional images of the target scatterers and the seabed. For this case, the first challenge was to develop forward modeling software that produced sufficiently accurate amplitudes as well as traveltimes in the forward propagating direction. An additional constraint for implementation is that the CPU time for forward modeling should be acceptable. The current code is highly accurate in both traveltime and phase for forward propagation, what is needed for the inverse problem. By smoothing the entire model, including known interfaces, a code running in acceptable CPU times was developed. We are currently experimenting with two methods for re-incorporate transmission coefficients into the modeling algorithm.

A crucial ingredient in keeping the CPU under control was the use of the so-called *wavefront construction method* for modeling the traveltimes. In this method, an appropriately dense set of rays is set off near the source. Triangular tiles on the wavefront are constructed from nearby rays. As the wave propagates forward, the sizes of the tiles and the opening angles between the edges of the tiles are recorded. When these numbers reach prescribed thresholds, new rays are added. In this manner, rays are only added as they are needed and the CPU for an adequate output model is kept to a minimum.

RESULTS

We show here an example of this forward modeling code applied to a section of the SEG/EAGE saltdome model, which is based on a typical US Gulf Coast salt structure. The complexity of the 3D salt structure makes it a benchmark model used to evaluate various 3D forward modeling and imaging algorithms. Scaling the distances down by a factor of 100 and scaling the frequencies up by the same factor provides an example of a hard structure in the near seabed. Figure 1 shows a set of rays from a point source. The velocity in the salt is about 4482 m/s, shown in black. The velocity of the host medium increases with depth, but is much lower than the velocity in the salt. The front face of this figure shows a vertical slice at x = 3.5km, which is 1.5km from the source. It passes through the salt structure. The rays were shot off with a uniform distribution of take-off angles. The feature of adding rays to maintain ray density was suppressed in this figure, so that we could see the relative distribution of the set of rays around the salt structure. Notice that the density of the post-critical rays that do not enter the salt is much higher than that of the rays that enter the salt and emerge through the front face. This indicates that we should expect the amplitude in the salt to be lower than the amplitude right above the salt. The waves that propagate through the salt generate first arrivals at near-salt and sub-salt regions. These waves dominate the solution of first arrival eikonal solvers.

Figure 2 is one wavefront recorded at 0.9 s with the source located at the center of the upper surface. Its lower part changes from the typical spherical shape, due to the presence of the high velocity salt. This structure causes portions of the wavefront to bulge and expand, especially those parts that have

penetrated the salt. The boundaries of this bulge are dominated by the pseudo-head-wave arrivals, which continuously connect the portions of the wavefront that penetrated the salt with those that traveled only through the sediments. However, head-waves are low-energy arrivals that are not useful for imaging applications. Waves traveling directly from the source, without going through the salt, carry more energy than rays that propagate through the salt.

Figure 3 is an amplitude plot on the same vertical slice as the front face of Figure 1. Here, the red and yellow colors indicate high amplitude and the purple color, low amplitude. The high and low amplitude zones agree with what we expected from the ray plot in Figure 1. From examples provided in earlier reports to ONR, we know that the amplitudes near turning are not as accurate as the transmitted amplitudes, but they are close enough qualitatively to confirm the agreement we see between these two figures.

As noted above, even the reflectors are smoothed in preparation for the ray tracing in order to generate stable amplitudes. Thus, it is necessary to insert transmission and reflection coefficients in a non-traditional manner. Here, we use a scheme that updates the transmission coefficients *pointwise.* That is, an approximate transmission coefficient is introduced at every step of the Runge-Kutta routine used for the ray tracing. Figure 4 depicts level curves of amplitude for a simple horizontal interface model, velocity, 2000m/s above, 2500m/s, below. The amplitude is generated from ray theory for the discontinuous model with level curves shown as solid curves. Then, the numerical output for the smoothed velocity model is generated, with level curves depicted with dashed curves. The numbers are the negative-log-amplitude. In this case, the transmission coefficient is equal to one. Thus, the method compares the close fit and stability of the ray-theory Jacobian calculations for the smoothed and discontinuous models. They are seen to agree extremely well in the forward propagation direction---exactly the direction of interest in the ultimate application to inversion. Figure 5 depicts the amplitudes again. However, now, the transmission coefficient is included in the analytically computed result and the pointwise generation of the transmission coefficient is included in the numerical modeling result produced by our code. Again, the agreement in the forward modeling direction is extremely good. Finally, we show a traveltime comparison in Figure 6. We can see the head wave produced by the analytic solution (solid curve) and the approximate head wave produced by the computer code (dashed curve). Except for the post-critical region, all of the amplitude and traveltime comparisons are accurate enough for proposed use in the inversion code.

IMPACT/APPLICATION

Inversion of towed array data under the assumption of a fully heterogeneous background wavespeed has resided in commercial processing companies servicing the oil industry and in the oil industry, itself. We know from our connections to the oil industry that the forward modeling program that we are developing is competitive with modeling programs available in the industry. Such forward modeling programs are the linchpins on which one builds a corresponding inversion code. Thus, we are developing code that will be generally available as free software through the Center for Wave Phenomena web site. We are aware of industrial codes available in the industry that have the imaging capability of the code that we are developing, but do not have the parameter estimation capability of our code.

TRANSITIONS

Our ties to the oil industry through a consortium of 30 companies provide a direct line for technology transfer and prompt and extensive testing of our science and its computer implementation. We know that our methods have led to industry-standard codes for processing seismic exploration data to aid in the identification of fluid traps in the Earth. Confirmation of the efficacy of our methods comes through annual renewal by our sponsors.

RELATED PROJECTS

In this program, we assume that the background wavespeed is known. Under other ONR support, we have developed a three dimensional *migration velocity analysis* method to help determine that background wavespeed. Also, there are standard preprocessing techniques designed to reduce the size and complexity of the data as well as to carry out preliminary analysis in advance of full 3D data processing. We have found that many of those methods fall in a single category that we call data mapping. This is a technique for transforming data from an input source/receiver configuration and presumed background earth model to a different source/receiver configuration and, possibly, a different earth model. This research was initiated under the now-defunct ACTI/DOE program. It is continuing under oil industry support through our consortium project. We are developing a theory that we call *Kirchhoff data mapping* (KDM). We have a general platform for this process and have developed implementations in the following list, with applicability and limitations as further implied by the titles in the references, below.

1. Mapping of data gathered at finite, fixed offset (common offset, bistatic) between source and receiver to zero offset (monostatic) data.
2. Downward continuation of receivers (or sources).
3. Mapping of common offset data to common shot data. This output, here provides synthetic data as if the receiver array were as long as the entire survey, rather than as long as the given towed array.

Other implementations are under development at this time. There is high interest in this subject in the oil industry.

REFERENCES

Wang, L., and Bleistein, N., 1998, 3D multi-valued traveltime and amplitude maps: Center for Wave Phenomena Report number CWP-278.

Meng, Z., 1999, Tetrahedral based earth models, ray tracing in tetrahedral models and analytical migration velocity analysis: Ph.D. thesis, Colorado School of Mines. (Mathematical and Computer Sciences.): Center for Wave Phenomena Report number CWP-296.

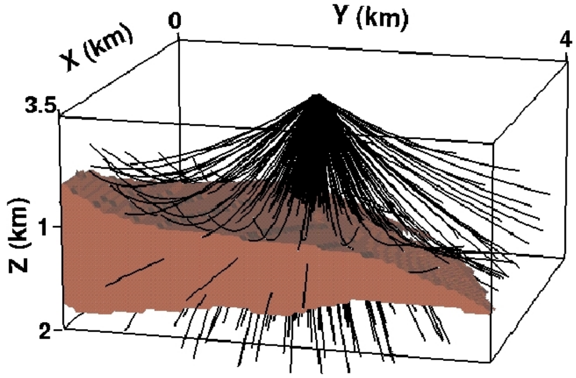

Figure 1. Rays from a point source propagating through a salt structure.

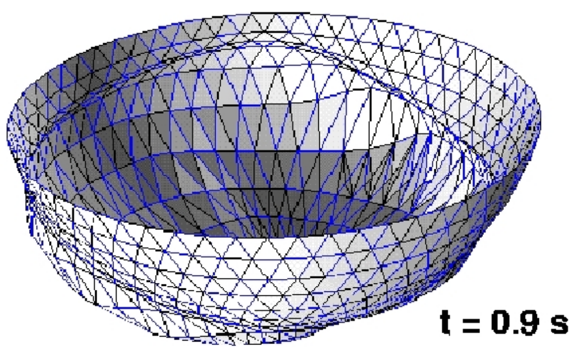

Figure 2. A wavefront or equal travel surface at .9 seconds.

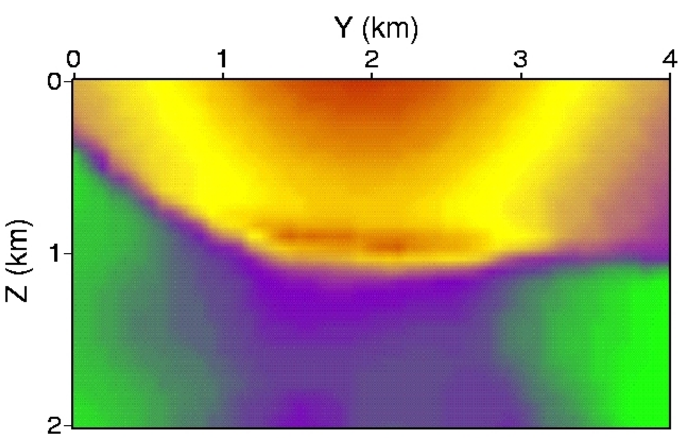

Figure 3. Amplitude plot on the same front face as in Figure 1.

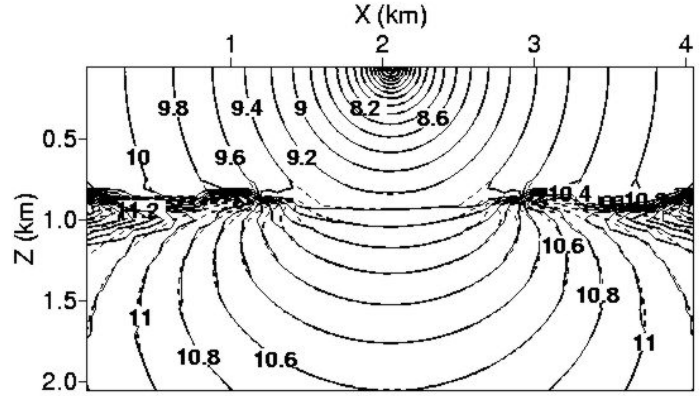

Figure 4. Amplitude comparison for horizontal interface model, velocity, 2000m/s (above), 2500m/s (below). Transmission coefficient = 1. Solid curve: ray theoretic amplitude for discontinuous medium; dashed curve: smoothed medium. Numbers: -log amplitude

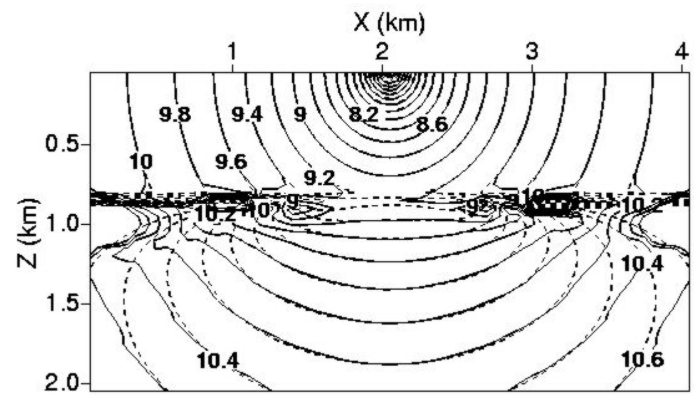

Figure 5. Amplitude comparison with true transmission coefficient.

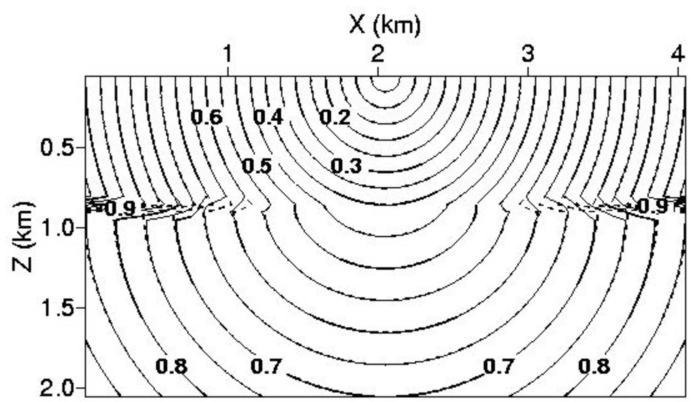

Figure 6. Traveltime comparison.